Space–time line coded regenerative two-way relay systems with power control

J. Joung, B.C. Jung and J. Choi✉

In this Letter, a general space–time line code (STLC)-based two-way relay (TWR) method is proposed to enable a power control for individual data streams transmitted to source nodes. Optimal power control factors are derived to ensure fairness between two source nodes under per-antenna power constraints. When the two-way channels are unbalanced, numerical results verify that the proposed method outperforms the existing TWR methods, an STLC TWR method without power control, and a space division multiple-access-based TWR method.

Introduction: A two-way relay (TWR) system effectively supports data exchange between two source nodes (SNs), called source nodes A and B (SnA and SnB), via a relay node (RN) within two phases. Various TWR schemes have been studied for low-complexity forwarding [1], cooperative relaying [2], relaying with a direct link [3], beamforming at RN [4], and precoding at RN [5]. A space–time line code (STLC) proposed in [6] has been applied to reduce peak-to-average-power ratio (PAPR) of a TWR in [7] with per-antenna power constraints (PAPCs) [8]. The per-antenna STLC can effectively reduce PAPR, inter-symbol interference (ISI), and self-interference (SI) as shown in [6]. However, the study in [6] was limited to the case when SnA-to-RN and SnB-to-RN links are balanced, i.e. the case when SnA and SnB are located at the same distance from the TWR.

In this Letter, we propose a power control (PC) method for the STLC-based regenerative (i.e. decode-and-forward) TWR system under general communication scenarios, in which the distance between SnA and RN differs from that between SnB and RN. It is verified that the superposition of two STLC encoding matrices is optimal in terms of maximising the detection signal-to-interference-plus-noise ratio (SINR) at each SN, which is not shown in [6]. Furthermore, an optimisation problem is formulated that maximises the product of SINRs for SnA and SnB with respect to PC factors, and a closed-form solution is derived. It is verified through numerical simulations that the proposed STLC-based TWR method is beneficial than conventional TWR schemes.

Notations: Superscripts T, H, and $*$ denote transposition, Hermitian transposition, and complex conjugate, respectively, for any scalar, vector, or matrix. $|\boldsymbol{x}|$ denotes the 2-norm of a vector $\boldsymbol{x}$; $\boldsymbol{I}_m$ and $\boldsymbol{0}_m$ represent an m-by-m identity and zero matrices, respectively; blkdiag$[\{\boldsymbol{A}\}_{m=1}^{M}]$ denotes a block-diagonal matrix composed of $\boldsymbol{A}_1, \ldots, \boldsymbol{A}_M$; and $x \sim \mathcal{CN}(0, \sigma^2)$ means a complex Gaussian random variable x with zero mean and variance σ^2. $E[x]$ stands for the expectation of x.

STLC-based TWR system model: Consider a TWR system, in which SnA and SnB with two antennas each exchange their data. SnA and SnB are apart from TWR by d_A and d_B, respectively. In the first phase, the SnA and SnB transmit symbol vectors $\boldsymbol{a} = [a_1, a_2]^{\mathrm{T}}$ and $\boldsymbol{b} = [b_1, b_2]^{\mathrm{T}}$, simultaneously, to a TWR with M antennas. Here, no direct link between SnA and SnB is considered due to the obstacles. The channels from the nth antennas of SnA and SnB to the mth antenna of RN are denoted as $h_{m,n} = \sqrt{\alpha_h}\bar{h}_{m,n}$ and $g_{m,n} = \sqrt{\alpha_g}\bar{g}_{m,n}$, respectively, where $n \in \{1, 2\}$ and $m \in \mathcal{M} = \{1, \ldots, M\}$; α_h and α_g are the large scaling factors between SnA and RN and between SnB and RN, respectively; and $\bar{h}_{m,n}$ and $\bar{g}_{m,n}$ are the small-scale fading channels, which are independent and identically distributed (i.i.d.) random variables with $\mathcal{CN}(0, 1)$. Considering a time division duplex TWR system, the channels from SNs to RN and from RN to SNs are assumed to be symmetric. Here, the channel state information (CSI) is assumed to be available at RN by estimating it during the first phase. The maximum power of the mth transmit antenna at RN is limited by P_m, accounting for per-antenna power constraints (PAPCs) [9].

In the first phase, the RN regenerates $\hat{\boldsymbol{a}}$ and $\hat{\boldsymbol{b}}$ for $\boldsymbol{a}$ and $\boldsymbol{b}$, respectively, and in the second phase, $\hat{\boldsymbol{a}}$ and $\hat{\boldsymbol{b}}$ are forwarded to SnB and SnA. To this end, the RN encodes $\hat{\boldsymbol{a}}$ and $\hat{\boldsymbol{b}}$ using the structure of STLC as follows:

$$\begin{bmatrix} s_{1,m}^* \\ s_{2,m} \end{bmatrix} = \sqrt{p_{A,m}} \begin{bmatrix} w_{1,m} & w_{2,m} \\ w_{2,m}^* & -w_{1,m}^* \end{bmatrix} \begin{bmatrix} \hat{b}_1^* \\ \hat{b}_2 \end{bmatrix} + \sqrt{p_{B,m}} \begin{bmatrix} v_{1,m} & v_{2,m} \\ v_{2,m}^* & -v_{1,m}^* \end{bmatrix} \begin{bmatrix} \hat{a}_1^* \\ \hat{a}_2 \end{bmatrix}, \tag{1}$$

where $s_{t,m}$ is the STLC symbol that is for the mth transmit antenna at time $t \in \{1,2\}$; $p_{A,m}$ and $p_{B,m}$ are the power dividing factors of the mth antenna for SnA and SnB, respectively, such that $p_{A,m} + p_{B,m} = 1$, for all $m \in \mathcal{M}$; and complex values $w_{n,m}$ and $v_{n,m}$ are the encoding weights for $\hat{\boldsymbol{b}}$ and $\hat{\boldsymbol{a}}$, respectively.

The RN then broadcasts $s_{1,m}$ and $s_{2,m}$ in (1) through the mth antenna at the first- and second-time slots, sequentially. Consequently, the received signal at the nth antenna of SnA and time slot t from all M antennas is written as [7]

$$y_{A,n,t} = \sum_{m \in \mathcal{M}} h_{n,m} s_{t,m} + z_{A,n,t}, \tag{2}$$

where $z_{A,n,t}$ is the corresponding additive white Gaussian noise (AWGN) with $\mathcal{CN}(0, \sigma^2)$. Similarly, the received signal at SnB can be modelled by using $g_{n,m}$.

STLC precoder design: We first derive the received SINRs at SnA and SnB, and then propose the STLC precoder to maximise the product of SINRs. The SnA combines the received signals in (2), i.e. STLC decoding as follows:

$$y_{A,1,1} + y_{A,2,2}^* = \boldsymbol{h}^{\mathrm{H}} \boldsymbol{P}_A \boldsymbol{w} \hat{b}_1 + \boldsymbol{h}^{\mathrm{H}} \boldsymbol{P}_A \boldsymbol{Q} \boldsymbol{w}^* \hat{b}_2^* \tag{3a}$$

$$+ \boldsymbol{h}^{\mathrm{H}} \boldsymbol{P}_B \boldsymbol{v} \hat{a}_1 + \boldsymbol{h}^{\mathrm{H}} \boldsymbol{P}_B \boldsymbol{Q} \boldsymbol{v}^* \hat{a}_2^* \tag{3b}$$

$$+ z_{A,1,1} + z_{A,2,2}^*, \tag{3c}$$

$$- y_{A,1,2} + y_{A,2,1}^* = \boldsymbol{h}^{\mathrm{H}} \boldsymbol{P}_A \boldsymbol{w} \hat{b}_2 - \boldsymbol{h}^{\mathrm{H}} \boldsymbol{P}_A \boldsymbol{Q} \boldsymbol{w}^* \hat{b}_1^* \tag{4a}$$

$$+ \boldsymbol{h}^{\mathrm{H}} \boldsymbol{P}_B \boldsymbol{v} \hat{a}_2 - \boldsymbol{h}^{\mathrm{H}} \boldsymbol{P}_B \boldsymbol{Q} \boldsymbol{v}^* \hat{a}_1^* \tag{4b}$$

$$- z_{A,1,2} + z_{A,2,1}^*, \tag{4c}$$

where $\boldsymbol{h} \triangleq [\boldsymbol{h}_1^T, \boldsymbol{h}_2^T, \ldots, \boldsymbol{h}_M^T]^{\mathrm{T}} \in \mathbb{C}^{2M \times 1}$, $\boldsymbol{h}_m \triangleq [h_{1,m}^*, h_{2,m}]^{\mathrm{T}} \in \mathbb{C}^{2 \times 1}$, $\boldsymbol{w} \triangleq [\boldsymbol{w}_1^T, \ldots, \boldsymbol{w}_M^T]^{\mathrm{T}} \in \mathbb{C}^{2M \times 1}$, $\boldsymbol{w}_m \triangleq [w_{1,m}^*, w_{2,m}]^{\mathrm{T}} \in \mathbb{C}^{2 \times 1}$, $\boldsymbol{P}_A \triangleq$ blkdiag$[\sqrt{p_{A,1}}\boldsymbol{I}_2 \cdots \sqrt{p_{A,M}}\boldsymbol{I}_2] \in \mathbb{R}^{2M \times 2M}$, $\boldsymbol{v} \triangleq [\boldsymbol{v}_1^T, \ldots, \boldsymbol{v}_M^T]^{\mathrm{T}} \in \mathbb{C}^{2M \times 1}$, $\boldsymbol{v}_m \triangleq [v_{1,m}^*, v_{2,m}]^{\mathrm{T}} \in \mathbb{C}^{2 \times 1}$, $\boldsymbol{P}_B \triangleq$ blkdiag$[\sqrt{p_{B,1}}\boldsymbol{I}_2 \cdots \sqrt{p_{B,M}}\boldsymbol{I}_2] \in \mathbb{R}^{2M \times 2M}$, $\boldsymbol{Q} \triangleq$ blkdiag$[\boldsymbol{Q}_2 \cdots \boldsymbol{Q}_2] \in \mathbb{R}^{2M \times 2M}$, and $\boldsymbol{Q}_2 = \left[\begin{smallmatrix} 0 & 1 \\ -1 & 0 \end{smallmatrix}\right]$.

Here, the first term of the right-hand side (RHS) in (3a) and (4a) is the intended signal; the second term of the RHS in (3a) and (4a) is ISI; (3b) and (4b) are SIs; and (3c) and (4c) are AWGNs.

Using the fact that information symbols are independent of ISIs, SIs, and AWGNs in (3a)–(3c) and (4a)–(4c), we can show that the SINRs for $\hat{b}_1$ and $\hat{b}_2$ are identical to each other and can derive the SINR for SnA, ρ_A, as follows:

$$\rho_A = \frac{|\boldsymbol{h}^{\mathrm{H}} \boldsymbol{P}_A \boldsymbol{w}|^2}{|\boldsymbol{h}^{\mathrm{H}} \boldsymbol{P}_A \boldsymbol{Q} \boldsymbol{w}^*|^2 + |\boldsymbol{h}^{\mathrm{H}} \boldsymbol{P}_B \boldsymbol{v}|^2 + |\boldsymbol{h}^{\mathrm{H}} \boldsymbol{P}_B \boldsymbol{Q} \boldsymbol{v}^*|^2 + 2\sigma_n^2}. \tag{5}$$

Similarly, the SINR after the combining at SnB is derived as follows:

$$\rho_B = \frac{|\boldsymbol{g}^{\mathrm{H}} \boldsymbol{P}_B \boldsymbol{v}|^2}{|\boldsymbol{g}^{\mathrm{H}} \boldsymbol{P}_B \boldsymbol{Q} \boldsymbol{v}^*|^2 + |\boldsymbol{g}^{\mathrm{H}} \boldsymbol{P}_A \boldsymbol{w}|^2 + |\boldsymbol{g}^{\mathrm{H}} \boldsymbol{P}_A \boldsymbol{Q} \boldsymbol{w}^*|^2 + 2\sigma_n^2}, \tag{6}$$

where $\boldsymbol{g} \triangleq [\boldsymbol{g}_1^T, \ldots, \boldsymbol{g}_M^T]^{\mathrm{T}} \in \mathbb{C}^{2M \times 1}$ and $\boldsymbol{g}_m \triangleq [g_{1,m}^*, g_{2,m}]^{\mathrm{T}} \in \mathbb{C}^{2 \times 1}$.

We now design the STLC precoder, namely $\boldsymbol{w}$ and $\boldsymbol{v}$, and PC factors $\{p_{A,m}, p_{B,m}\}$, such that the product of SINRs are maximised. Note that a max–min optimisation of ρ_A and ρ_B is required to rigorously ensure fairness between SnA and SnB. However, the max–min optimisation cannot be solved in a closed form. To obtain a more tractable solution, we have considered the product-SINR maximisation problem. Under transmit power constraints, the product-SINR $\rho_A \rho_B$ tends to be maximised when ρ_A is similar to ρ_B, and thus the fairness between SnA and SnB is guaranteed as in the max–min optimisation problem. Moreover, the maximisation of the product SINR is aligned to maximise the sum rate of TWR systems in the high SINR region. Using (5) and (6), the product-SINR maximisation problem finding $\{\boldsymbol{w}, \boldsymbol{v}, \boldsymbol{P}_A, \boldsymbol{P}_B\}$ is formulated as follows:

$$\begin{aligned} \max_{\boldsymbol{w}, \boldsymbol{v}, \boldsymbol{P}_A, \boldsymbol{P}_B} \quad & \rho_A \rho_B \\ \text{s.t.} \quad & p_{A,m} |\boldsymbol{w}_m|^2 + p_{B,m} |\boldsymbol{v}_m|^2 \le P_m, \quad \forall m \in \mathcal{M}, \\ & p_{A,m} + p_{B,m} = 1, \end{aligned} \tag{7}$$

where the first constraints denote PAPCs obtained from $E|s_{t,m}|^2 \le P_m$, $\forall m \in \mathcal{M}$.

To find the optimal solution of (7), we derive the following property:

$$|\boldsymbol{h}^{\mathrm{H}}\boldsymbol{P}_B\boldsymbol{v}|^2+|\boldsymbol{h}^{\mathrm{H}}\boldsymbol{P}_B\boldsymbol{Q}\boldsymbol{v}^*|^2=\boldsymbol{h}^{\mathrm{H}}\boldsymbol{P}_B\left(\boldsymbol{v}\boldsymbol{v}^{\mathrm{H}}+\boldsymbol{Q}^T\boldsymbol{v}^*\boldsymbol{v}^T\boldsymbol{Q}\right)\boldsymbol{P}_B\boldsymbol{h}$$
$$=\boldsymbol{h}^{\mathrm{H}}\boldsymbol{P}_B\begin{bmatrix}|\boldsymbol{v}|^2 & 0\\ 0 & |\boldsymbol{v}|^2\end{bmatrix}\boldsymbol{P}_B\boldsymbol{h}=|\boldsymbol{h}\boldsymbol{P}_B|^2|\boldsymbol{v}|^2. \tag{8}$$

Similarly, we obtain that $|\boldsymbol{g}^{\mathrm{H}}\boldsymbol{P}_A\boldsymbol{w}|^2+|\boldsymbol{g}^{\mathrm{H}}\boldsymbol{P}_A\boldsymbol{Q}\boldsymbol{w}^*|^2=|\boldsymbol{g}\boldsymbol{P}_A|^2|\boldsymbol{w}|^2$ for ρ_B. By substituting these properties into (5) and (6), the upper bound of the objective function in (7) is expressed as

$$\rho_A\rho_B\underset{\le}{(\mathrm{a})}\frac{|\boldsymbol{h}^{\mathrm{H}}\boldsymbol{P}_A\boldsymbol{w}|^2|\boldsymbol{g}^{\mathrm{H}}\boldsymbol{P}_B\boldsymbol{v}|^2}{\left(|\boldsymbol{h}\boldsymbol{P}_A|^2|\boldsymbol{v}|^2+2\sigma_n^2\right)\left(|\boldsymbol{g}\boldsymbol{P}_B|^2|\boldsymbol{w}|^2+2\sigma_n^2\right)}$$
$$\underset{\le}{(\mathrm{b})}\frac{|\boldsymbol{h}|^2|\boldsymbol{P}_A\boldsymbol{w}|^2|\boldsymbol{g}|^2|\boldsymbol{P}_B\boldsymbol{v}|^2}{\left(|\boldsymbol{h}\boldsymbol{P}_A|^2|\boldsymbol{v}|^2+2\sigma_n^2\right)\left(|\boldsymbol{g}\boldsymbol{P}_B|^2|\boldsymbol{w}|^2+2\sigma_n^2\right)}, \tag{9}$$

where the equality (a) holds if

$$\boldsymbol{h}^{\mathrm{H}}\boldsymbol{P}_A\boldsymbol{Q}\boldsymbol{w}^*=0\ \text{ and }\ \boldsymbol{g}^{\mathrm{H}}\boldsymbol{P}_B\boldsymbol{Q}\boldsymbol{v}^*=0, \tag{10}$$

and the equality (b) holds if

$$\boldsymbol{w}=\boldsymbol{C}_1\boldsymbol{P}_A^{-1}\boldsymbol{h}\ \text{ and }\ \boldsymbol{v}=\boldsymbol{C}_2\boldsymbol{P}_B^{-1}\boldsymbol{g}. \tag{11}$$

Here, $\boldsymbol{C}_k=\mathrm{blkdiag}[c_{k,1}\boldsymbol{I}_2,c_{k,2}\boldsymbol{I}_2,\ldots,c_{k,M}\boldsymbol{I}_2]$ for arbitrary real values $\{c_{k,m};k\in\{1,2\},m\in\mathcal{M}\}$.

Now, it can be readily shown that $\boldsymbol{w}$ and $\boldsymbol{v}$ in (11) fulfil (10). Thus, the optimal STLC precoding vectors can be defined for each antenna from (11) as below:

$$\boldsymbol{w}_m=c_{1,m}p_{A,m}^{-1/2}\boldsymbol{h}_m\ \text{ and }\ \boldsymbol{v}_m=c_{2,m}p_{B,m}^{-1/2}\boldsymbol{g}_m,\quad\forall m\in\mathcal{M}. \tag{12}$$

Since the upper bound in (9) is clearly an increasing function with respect to $c_{1,m}$ and $c_{2,m}$, the maximum transmit power is used in each antenna. Thus, $c_{1,m}$ and $c_{2,m}$ are designed from the constraints of (7) as follows:

$$c_{1,m}=\sqrt{P_m/(2|\boldsymbol{h}_m|^2)}\ \text{ and }\ c_{2,m}=\sqrt{P_m/(2|\boldsymbol{g}_m|^2)}. \tag{13}$$

Substituting (12) and (13) into (1), we obtain the optimal STLC encoder maximising product-SINR under PAPCs as follows ($\forall m\in\mathcal{M}$):

$$\begin{bmatrix}s_{1,m}^*\\ s_{2,m}\end{bmatrix}=\sqrt{\frac{P_m}{2|\boldsymbol{h}_m|^2}}\begin{bmatrix}h_{1,m} & h_{2,m}\\ h_{2,m}^* & -h_{1,m}^*\end{bmatrix}\begin{bmatrix}\hat{b}_1^*\\ \hat{b}_2\end{bmatrix}$$
$$+\sqrt{\frac{P_m}{2|\boldsymbol{g}_m|^2}}\begin{bmatrix}g_{1,m} & g_{2,m}\\ g_{2,m}^* & -g_{1,m}^*\end{bmatrix}\begin{bmatrix}\hat{a}_1^*\\ \hat{a}_2\end{bmatrix}. \tag{14}$$

Contrary to the STLC-TWR scheme in [6], the proposed STLC scheme in (14) adjusts the PC factors according to the corresponding two-way link gains, i.e. $|\boldsymbol{h}_m|^2$ and $|\boldsymbol{g}_m|^2$ as concretely as follows:

$$p_{A,m}=\frac{P_m}{2|\boldsymbol{h}_m|^2}\ \text{ and }\ p_{B,m}=\frac{P_m}{2|\boldsymbol{g}_m|^2}. \tag{15}$$

This individual PC can mitigate significant unbalancing problem when the two-way links are asymmetric. Note that the decoding procedure at SnA and SnB is the same as that of the conventional STLC in [7].

CSI uncertainty and computational complexity analysis: The effect of CSI error in the STLC encoding and decoding scheme has been rigorously evaluated in [7]. The SDMA scheme [5] uses a zero-forcing-based precoding based on singular value decomposition (SVD) in order to remove the inter-stream interference. In contrast, the STLC without PC [7] and the proposed STLC method maximise the detection SINRs at SnA and SnB in the minimum mean square error sense, allowing some level of inter-stream interference. Thus, it is obvious that the STLC-based methods are more advantageous than the SDMA scheme. Moreover, since the STLC in [7] and the proposed method use the same receiver structure, the influence of CSI error is identical to each other.

The computational complexity is compared in terms of the number of complex operations including addition and multiplication. The SDMA scheme finds precoding matrices using SVD for nulling of inter-stream interference and performs linear precoding, requiring $4M^2$ [10] and $14M$ operations, respectively, for transmission during two symbol intervals. On the other hand, the STLC without PC necessitates $18M$ operations and the proposed method requires $20M$ operations. Overall, the proposed method has a similar computational load to the STLC without PC, and needs much less computational complexity than the SDMA scheme when M is large.

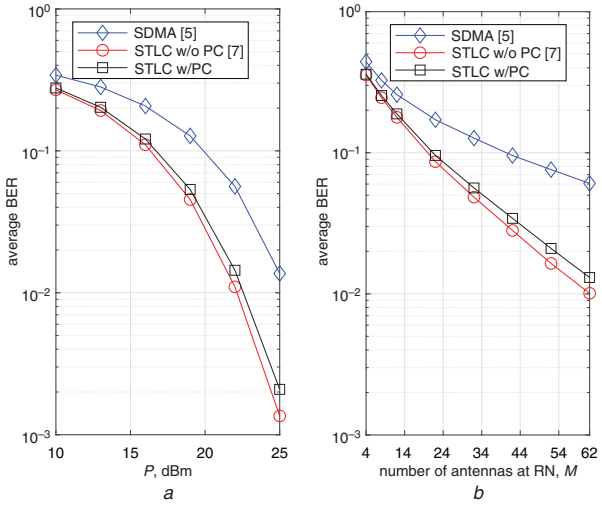

Fig. 1 *Average BER of SnA and SnB*
a When $M=40$, $d_A=500$ m, and $d_B=500$ m
b When $P=20$ dBm, $d_A=500$ m, and $d_B=500$ m

Performance evaluation and comparison: To justify the proposed STLC-based TWR method, the bit error rate (BER) performance is evaluated. For comparison, we consider the SDMA-based TWR method (see [5] for details) and the STLC-based TWR scheme without PC in [6]. Since we are focusing on the second-phase performance, a space–time block code is commonly used during the first phase transmission for all TWR schemes. As reported in [6], the spectral efficiency of the STLC-based method is half that of the SDMA-based method. Thus, for a fair comparison of the STLC- and SDMA-based TWR methods in the second phase, the STLC-based RN forwards the regenerated quadrature phase-shift keying (QPSK) symbols to SNs, while the SDMA-based RN forwards binary phase-shift keying (BPSK) symbols to SNs. In our simulation, it is assumed that the large scaling fading factors are determined by the path losses which are given by $\alpha_h=-23.4+10\log_{10}(d_A^{-\mu})$ and $\alpha_g=-23.4+10\log_{10}(d_B^{-\mu})$ on dB scale, where the path loss exponent is set to $\mu=3.76$, d_A is the distance between RN and SnA, d_B is the distance between RN and SnB; and the small-scale channels are modelled as $\bar{h}_{n,m}\sim\mathcal{CN}(0,1)$ and $\bar{g}_{n,m}\sim\mathcal{CN}(0,1)$. The maximum power of all transmit antennas is set to be identical, i.e. $P\triangleq P_1=\cdots=P_M$. Furthermore, the transmit signal is clipped using the soft-limiter model of a non-linear power amplifier in [11], and the noise figure is set to -174 dBm.

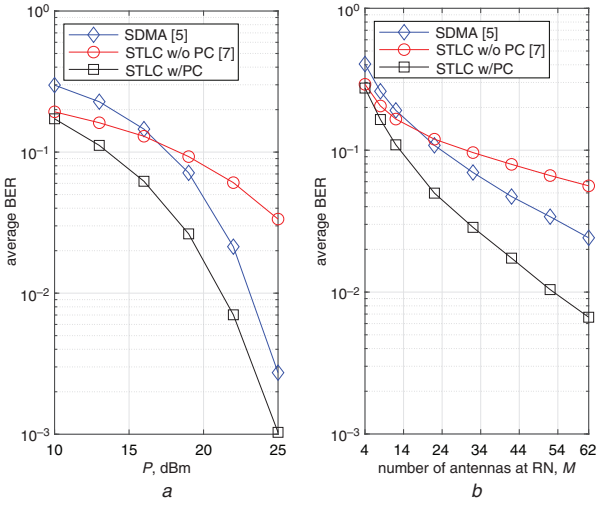

Fig. 2 *Average BER of SnA and SnB*
a When $M=40$, $d_A=300$ m, and $d_B=500$ m
b When $P=20$ dBm, $d_A=300$ m, and $d_B=500$ m

When $d_A = 500$ m and $d_B = 500$ m, i.e. the two links are balanced, the average BER of SnA and SnB is evaluated across P dBm for $M = 40$ in Fig. 1*a*, and across M for $P = 20$ dBm in Fig. 1*b*, respectively. Fig. 1 presents that the conventional STLC-based TWR in [6] can achieve the best BER performance. Here, the proposed STLC encoder in (14) performs comparable to the conventional STLC-based method. We now evaluate the average BER performance when $d_A = 300$ m, and $d_B = 500$ m, i.e. the two links are unbalanced. Here, the BER performance is evaluated across P dBm for $M = 40$ in Fig. 2*a*, and across M for $P = 20$ dBm in Fig. 2*b*, respectively. As shown in Fig. 2, the BER performance of the conventional STLC-based TWR is deteriorated and inferior to the proposed STLC-based TWR method. Note that the conventional STLC-based TWR employs a common power factor regardless of the difference of two-way link gains. However, the proposed STLC encoder in (14) allows a PC according to the link gains, i.e. the smaller weight for the larger-gain link and the larger weight for the smaller-gain link, which intuitively balances the asymmetric two-way links. Thus, the proposed method provides the significant BER performance improvement, regardless of P and M.

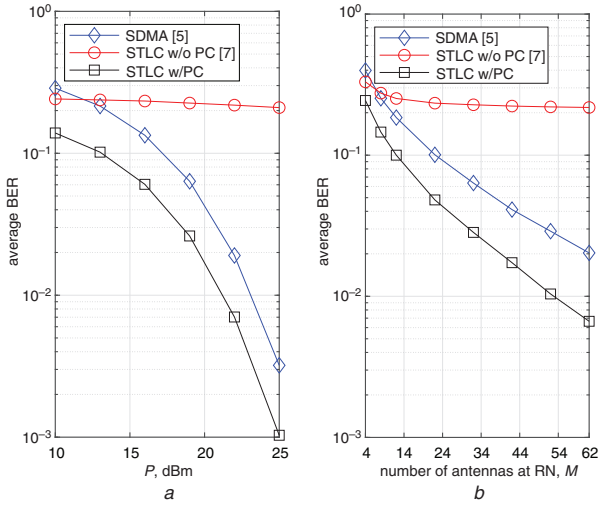

Fig. 3 *Average BER of SnA and SnB*
a When $M = 40$, $d_A = 100$ m, and $d_B = 500$ m
b When $P = 20$ dBm, $d_A = 100$ m, and $d_B = 500$ m

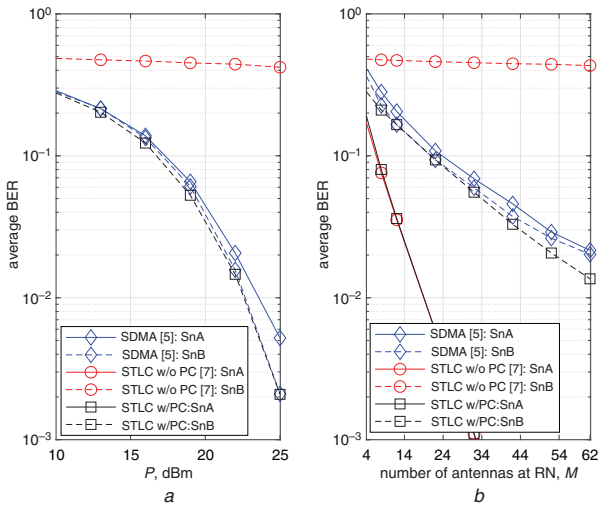

Fig. 4 *Individual BER of SnA and SnB*
a When $M = 40$, $d_A = 100$ m, and $d_B = 500$ m
b When $P = 20$ dBm, $d_A = 100$ m, and $d_B = 500$ m

When the two links are highly unbalanced as $d_A = 100$ m and $d_B = 500$ m, the average BER performance is evaluated across P dBm for $M = 40$ in Fig. 3*a*, and across M for $P = 20$ dBm in Fig. 3*b*, respectively. Fig. 3 shows that the conventional STLC-based TWR has very poor BER performance. As mentioned before, the conventional STLC-based TWR does not consider the unbalanced gains between two links, the average BER performance is very poor. This is also verified in Fig. 4 that presents the individual BER values of SnA and SnB. As expected, the conventional STLC-based TWR system has highly unbalanced BER values for SnA and SnB. Note that no error is observed at SnA of the STLC-based TWR systems in Fig. 4*a*. However, the BERs of SnA and SnB are relatively balanced from the proposed STLC with PC compared to the conventional STLC-based TWR as shown in Fig. 4. Overall, the proposed STLC encoder in (14) provides the best average BER performance regardless of P and M.

Conclusion: In this Letter, a general STLC-based TWR method with individual power control for SNs is proposed. Under PAPCs, the proposed method outperforms the existing methods, i.e. an STLC-based TWR method without PC for two data streams and an SDMA-based TWR method. Rigorous simulation results verify that the proposed method achieves BER performance improvement, especially, at low BER regime, regardless of the distribution of SNs, the number of RN antennas, and the transmit power of RN.

Acknowledgments: This research was supported by the National Research Foundation of Korea (NRF) grant funded by the Korea government (MSIT) (2018R1A4A1023826).

Submitted: *12 February 2019* E-first: *15 May 2019*
doi: 10.1049/el.2019.0541
One or more of the Figures in this Letter are available in colour online.

J. Joung (*School of Electrical and Electronics Engineering, Chung-Ang University, Seoul 06974, Republic of Korea*)

B.C. Jung (*Department of Electronics Engineering, Chungnam National University, Daejeon 34134, Republic of Korea*)

J. Choi (*School of Electronics and Information Engineering, Korea Aerospace University, Goyang-City, Gyeonggi-do 10540, Republic of Korea*)

✉ E-mail: jihoon@kau.ac.kr

References

1 Zhou, Q.F., Mow, W.H., Zhang, S., *et al.*: 'Two-way decode-and-forward for low-complexity wireless relaying: selective forwarding versus one-bit soft forwarding', *Trans. Wirel. Commun.*, 2016, **15**, (3), pp. 1866–1880
2 Li, C., Yang, H.J., Sun, F., *et al.*: 'Multiuser overhearing for cooperative two-way multiantenna relays', *Trans. Veh. Technol.*, 2016, **65**, (5), pp. 3796–3802
3 Pinals, L., and Vu, M.: 'Link-state optimized decode-forward transmission for two-way relaying', *Trans. Commun.*, 2016, **64**, (5), pp. 1844–1860
4 Joung, J.: 'Beamforming vector design for regenerative wired two-way relay systems', *IET Electron. Lett.*, 2017, **53**, (9), pp. 596–598
5 Joung, J., and Choi, J.: 'Linear precoder design for an AF two-way MIMO relay node with no source node precoding', *Trans. Veh. Technol.*, 2017, **66**, (11), pp. 10526–10531
6 Joung, J.: 'Space–time line code', *Access*, 2018, **6**, pp. 1023–1041
7 Joung, J.: 'Energy efficient space-time line coded regenerative two-way relay under per-antenna power constraints', *Access*, 2018, **6**, pp. 47026–47035
8 Choi, J., Han, S., and Joung, J.: 'Low complexity precoder design for multiuser MIMO systems with per-antenna power constraints', *Trans. Veh. Technol.*, 2018, **67**, (9), pp. 9011–9015
9 Dong, M., Liang, B., and Xiao, Q.: 'Unicast multi-antenna relay beamforming with per-antenna power control: optimization and duality', *Trans. Signal Process.*, 2013, **61**, (23), pp. 6076–6090
10 Golub, G.H., and Van Loan, C.F.: 'Matrix computation' (The Johons Hopkins University Press, MD, 1996, 3rd edn.)
11 Joung, J., Ho, C.K., Adachi, K., and Sun, S.: 'A survey on power-amplifier-centric techniques for spectrum and energy efficient wireless communications', *Commun. Surv. Tutor.*, 2014, **17**, (1), pp. 315–333